Autonomous refuelling mission in subarctic conditions

Dominic Baril[*]
Norlab, Université Laval
Québec, QC, Canada G1V 0A6
`dominic.baril@norlab.ulaval.ca`

Simon-Pierre Deschênes
Norlab, Université Laval
Québec, QC, Canada G1V 0A6

Olivier Gamache
Norlab, Université Laval
Québec, QC, Canada G1V 0A6

Maxime Vaidis
Norlab, Université Laval
Québec, QC, Canada G1V 0A6

Damien Larocque
Norlab, Université Laval
Québec, QC, Canada G1V 0A6

Johann Laconte
Norlab, Université Laval
Québec, QC, Canada G1V 0A6

Vladimír Kubelka
Norlab, Université Laval
Québec, QC, Canada G1V 0A6

Philippe Giguére
Norlab, Université Laval
Québec, QC, Canada G1V 0A6

François Pomerleau
Norlab, Université Laval
Québec, QC, Canada G1V 0A6
`francois.pomerleau@norlab.ulaval.ca`

Abstract

Lorem ipsum dolor sit amet, consectetuer adipiscing elit. Ut purus elit, vestibulum ut, placerat ac, adipiscing vitae, felis. Curabitur dictum gravida mauris. Nam arcu libero, nonummy eget, consectetuer id, vulputate a, magna. Donec vehicula augue eu neque. Pellentesque habitant morbi tristique senectus et netus et malesuada fames ac turpis egestas. Mauris ut leo. Cras viverra metus rhoncus sem. Nulla et lectus vestibulum urna fringilla ultrices. Phasellus eu tellus sit amet tortor gravida placerat. Integer sapien est, iaculis in, pretium quis, viverra ac, nunc. Praesent eget sem vel leo ultrices bibendum. Aenean faucibus. Morbi dolor nulla, malesuada eu, pulvinar at, mollis ac, nulla. Curabitur auctor semper nulla. Donec varius orci eget risus. Duis nibh mi, congue eu, accumsan eleifend, sagittis quis, diam. Duis eget orci sit amet orci dignissim rutrum.

1   Introduction

Lorem ipsum dolor sit amet, consectetuer adipiscing elit. Ut purus elit, vestibulum ut, placerat ac, adipiscing vitae, felis. Curabitur dictum gravida mauris. Nam arcu libero, nonummy eget, consectetuer id, vulputate a, magna. Donec vehicula augue eu neque. Pellentesque habitant morbi tristique senectus et netus et malesuada fames ac turpis egestas. Mauris ut leo. Cras viverra metus rhoncus sem. Nulla et lectus vestibulum urna fringilla ultrices. Phasellus eu tellus sit amet tortor gravida placerat. Integer sapien est, iaculis in, pretium quis, viverra ac, nunc. Praesent eget sem vel leo ultrices bibendum. Aenean faucibus. Morbi dolor nulla, malesuada eu, pulvinar at, mollis ac, nulla. Curabitur auctor semper nulla. Donec varius orci eget risus. Duis nibh mi, congue eu, accumsan eleifend, sagittis quis, diam. Duis eget orci sit amet orci dignissim rutrum.

---

[*]Use footnote for providing further information about author (webpage, alternative address). Acknowledgments to funding agencies should go in the **Acknowledgments** section at the end of the paper.
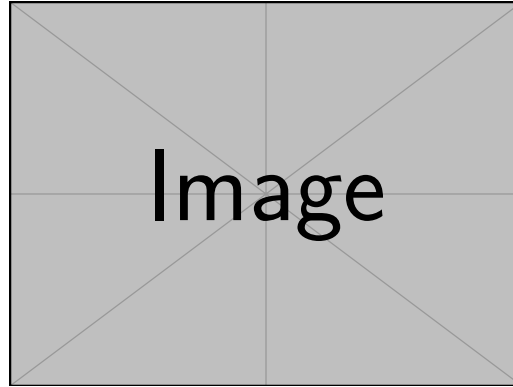
Figure 1: Warthog driving / Aerial shot of the different paths

Lorem ipsum dolor sit amet, consectetuer adipiscing elit. Ut purus elit, vestibulum ut, placerat ac, adipiscing vitae, felis. Curabitur dictum gravida mauris. Nam arcu libero, nonummy eget, consectetuer id, vulputate a, magna. Donec vehicula augue eu neque. Pellentesque habitant morbi tristique senectus et netus et malesuada fames ac turpis egestas. Mauris ut leo. Cras viverra metus rhoncus sem. Nulla et lectus vestibulum urna fringilla ultrices. Phasellus eu tellus sit amet tortor gravida placerat. Integer sapien est, iaculis in, pretium quis, viverra ac, nunc. Praesent eget sem vel leo ultrices bibendum. Aenean faucibus. Morbi dolor nulla, malesuada eu, pulvinar at, mollis ac, nulla. Curabitur auctor semper nulla. Donec varius orci eget risus. Duis nibh mi, congue eu, accumsan eleifend, sagittis quis, diam. Duis eget orci sit amet orci dignissim rutrum.

Lorem ipsum dolor sit amet, consectetuer adipiscing elit. Ut purus elit, vestibulum ut, placerat ac, adipiscing vitae, felis. Curabitur dictum gravida mauris. Nam arcu libero, nonummy eget, consectetuer id, vulputate a, magna. Donec vehicula augue eu neque. Pellentesque habitant morbi tristique senectus et netus et malesuada fames ac turpis egestas. Mauris ut leo. Cras viverra metus rhoncus sem. Nulla et lectus vestibulum urna fringilla ultrices. Phasellus eu tellus sit amet tortor gravida placerat. Integer sapien est, iaculis in, pretium quis, viverra ac, nunc. Praesent eget sem vel leo ultrices bibendum. Aenean faucibus. Morbi dolor nulla, malesuada eu, pulvinar at, mollis ac, nulla. Curabitur auctor semper nulla. Donec varius orci eget risus. Duis nibh mi, congue eu, accumsan eleifend, sagittis quis, diam. Duis eget orci sit amet orci dignissim rutrum.

Lorem ipsum dolor sit amet, consectetuer adipiscing elit. Ut purus elit, vestibulum ut, placerat ac, adipiscing vitae, felis. Curabitur dictum gravida mauris. Nam arcu libero, nonummy eget, consectetuer id, vulputate a, magna. Donec vehicula augue eu neque. Pellentesque habitant morbi tristique senectus et netus et malesuada fames ac turpis egestas. Mauris ut leo. Cras viverra metus rhoncus sem. Nulla et lectus vestibulum urna fringilla ultrices. Phasellus eu tellus sit amet tortor gravida placerat. Integer sapien est, iaculis in, pretium quis, viverra ac, nunc. Praesent eget sem vel leo ultrices bibendum. Aenean faucibus. Morbi dolor nulla, malesuada eu, pulvinar at, mollis ac, nulla. Curabitur auctor semper nulla. Donec varius orci eget risus. Duis nibh mi, congue eu, accumsan eleifend, sagittis quis, diam. Duis eget orci sit amet orci dignissim rutrum.

2 Related work

2.1 Robotic deployments in snow

To our knowledge, few robots have been deployed in harsh winter environments. Dante II is a $900\,\mathrm{kg}$ tethered legged robot, which conducted a 5-day, $165\,\mathrm{m}$ descent into the Mount Spurr Volcano, in Alaska (Bares & Wettergreen, 1999). During this deployment, Dante II reached speeds upwards to $0.011\,\mathrm{m/s}$ during the descent. A two-axis lidar was used to create a local elevation map around the robot in order to conduct autonomous navigation.

Nomad is a gasoline-powered $725\,\mathrm{kg}$ unmanned ground vehicle (UGV), was deployed at Elephant Moraine, Antarctica for a duration of 4 weeks (Apostolopoulos et al., 2000). The robot reached speeds upwards of $0.5\,\mathrm{m/s}$ while using differential-Global Positioning System (GPS) as the primary method of localization. The platform also used stereo cameras and a lidar sensor for obstacle detection, although stereo vision was found to be ineffective on blue ice and snow in Antarctica due to extreme lack of texture (Moorehead, Simmons, Apostolopoulos, & Whittaker, 1999). Roll/pitch/yaw sensors were also added to the robot to make it cognizant to hazardous terrain. Nomad achieved its initial goal to identify meteorites autonomously in Antarctica at a search rate of $160\,\mathrm{m^2/h}$.

MARVIN I and MARVIN II are two diesel-powered Skid-steering mobile robots (SSMRs) weighing $720\,\mathrm{kg}$ were deployed in Greenland (Stansbury, Akers, Harmon, & Agah, 2004) and Antarctica (Gifford, Akers, Stansbury, & Agah, 2009) respectively. The goal of these robots was to increase survey safety in remote polar regions and large sensor payloads led to the selection of large vehicles. Both vehicles used Real-time Kinematics (RTK) GPS as primary method, achieving a centimeter-level accuracy. They also used a lidar sensor for obstacle detection and a gyroscope and inclinometer were used to provide the robot's pitch and roll angles. Skid-steer turns often caused MARVIN I to get immobilized in snow and its transmission eventually broke down during operation. MARVIN II thus incorporated design improvements to the hydro-static drive and track systems to increase its durability.

Sno-mote Mk1 and Mk2 are dual-drive 1:10 scale snowmobiles equipped with a single camera and GPS antenna were deployed on Alaskan glaciers and Wapekoneta, Ohio (Williams & Howard, 2009). These robots were used to conduct manually-driven traverses of about $100\,\mathrm{m}$ at a speed of $1\,\mathrm{m/s}$. The data gathered with the Sno-motes was then used to improve visual Simultaneous Localization and Mapping (SLAM) feature extraction methods in snow. Despite improving feature detection methods on snow, it was shown that snow is still feature-sparse (Williams & Howard, 2009). Through this work, improvements were also done on slope estimation (Williams & Howard, 2010) and horizon line estimation (Williams & Howard, 2011).

Yeti is a battery-powered $81\,\mathrm{kg}$ UGV in Antarctica and Greenland (Lever et al., 2013). Yeti was used to conduct ground penetrating radar (GPR) surveys in order to detect subsurface crevasses or other voids to increase vehicle travel safety in remote polar environments. Since polar terrain is largely obstacle-free and the effort required to provide reliable obstacle detection on low-contrast snowfields is considerable, Yeti drove "blind", relying only on GPS waypoint following. During surveys, Yeti reached a top speed of $2.2\,\mathrm{m/s}$ and managed to acquire data on hundreds of crevasse encounters and even locate a previously undetected buried building in the South Pole.

A Clearpath Robotics Grizzly, a battery- and gasoline-powered SSMR was deployed during winter on the University of Toronto Institute for Aerospace Studies (UTIAS) campus, in Ontario, Canada (Paton, Pomerleau, MacTavish, Ostafew, & Barfoot, 2017). Only stereo cameras were used through a visual SLAM algorithm to localize the robot during autonomous teach-and-repeat runs. Path tracking was accomplished using a Model Predictive Control (MPC) algorithm. A 250 m path was successfully repeated on a light snow cover 3 hours after it was first manually driven. However, deep snow path-following provided unsatisfactory results due to features almost only being observed on the horizon, leading to inaccurate pose estimates, which caused issues for the path tracker. Furthermore, vehicle tracks that constantly change when driven over lead to an increased pose estimation error.

A full-scale battery-powered Toyota Prius was deployed during winter on roads in Massachusetts, USA (Ort, Gilitschenski, & Rus, 2020). Localization was accomplished using a custom-designed localizing GPR. A prior mapping must be conducted during which the driven is driven by a human operator and the vehicle's sensor data is recorded, the saved map can then allow the vehicle to localize within this area. The GPR location information is then probabilistically fused with wheel odometry and inertial measurement unit (IMU) measurements to provide accurate vehicle localization. Path tracking is accomplished through the use of a Pure Pursuit controller, specifically designed for Ackermann steered autonomous vehicles. The system showed similar performance in localization accuracy ($0.34\,\mathrm{m}$ to $0.39\,\mathrm{m}$) and cross-track error ($0.26\,\mathrm{m}$ to $0.29\,\mathrm{m}$) between clear weather and snow-covered road. The localizing GPR sensor's measurement range depends on the width of the array, meaning the system cannot be easily miniaturized, which means it was mounted on the rear of the vehicle, at $32\,\mathrm{cm}$ above the ground. This sensor size and mounting requirement could lead to decreased performance in deep snow or in off-road environments.

In this work, we demonstrate that lidar-based localization and navigation allows a robot to localize in Global Navigation Satellite System (GNSS)-deprived areas as well in snow-covered terrain. Our system has been deployed in complex meteorological scenarios, relying on lidar, IMU and wheel encoders measurements to localize and track the desired path through a week-long deployment in a subarctic forest.

2.2 Teach-and-Repeat

In Visual Teach and Repeat (VT&R), a robot is first driven manually along a given path as a training example in order to build a manifold map of overlapping submaps. Then, a visual path-tracking system is able to achieve high autonomy rates over many kilometers of steep terrain, relying on a single stereo camera (Furgale & Barfoot, 2010). Experience-based navigation (EBN) has then been introduced to increase the robustness of VT&R to scene appearance change, caused by illumination variation or dynamic environment changes (Churchill & Newman, 2013). This feature was added in VT&R through Multi-experience Localization (MEL), with the added ability to use landmarks from previous experiences in the same localization problem (Paton, MacTavish, Warren, & Barfoot, 2016). Recall of relevant landmarks for a specific scenario was then improved in computation speed through a bag-of-word approach (MacTavish, Paton, & Barfoot, 2017). To mitigate the impact of illumination variations, color-constant image transformations have been added to VT&R (Paton, MacTavish, Ostafew, & Barfoot, 2015). The VT&R framework has also been shown to work with various sensors, such as intensity-based lidar (McManus, Furgale, Stenning, & Barfoot, 2013) and monocular cameras (Clement, Kelly, & Barfoot, 2017). Convolutional Neural Networks (CNNs) and particle filters have also been used for visual place recognition in VT&R frameworks in order to localize the robot in the taught trajectory (Camara et al., 2020). In this work, the horizontal offset of the reference image with the current image is used to correct the steering during the teach phase. Recently, Congram and Barfoot (2021) expanded VT&R's localization ability to environments where the ability to visually localize is compromised by using GNSS measurements. While VT&R has proven to be an efficient method for repeating trajectories in outdoor environments, the literature does not show the system to be deployed in snow. Our work aims to demonstrate that Lidar Teach and Repeat (LT&R) approaches allow repeating trajectories that were recorded multiple days prior and under vastly different lighting conditions. We also demonstrate that LT&R offers good performance on snow-covered terrain, which is known to be complex for visual localization.

While all these works rely on using cameras, LT&R is a similar framework relying on lidar sensors. Marshall, Barfoot, and Larsson (2008) were the first to suggest a similar framework using encoders and 2D lidars. In this work, a sequence of overlapping metric maps are recorded along the path using 2D lidar measurements to allow the robot to localize within during the repeat phase. Sprunk, Tipaldi, Cherubini, and Burgard (2013) used a similar approach to LT&R, however the teach phase directly logs 2D lidar data at an interval based on the distance from the last recorded scan. Mazuran, Sprunk, Burgard, and Tipaldi (2015) have improved this framework by introducing an optimization step between the teach and the repeat phase, allowing the constraints to be defined by user preferences. While more focused on localization, Landry and Giguère (2016) have worked to improve topometric maps used to localize the robot during the repeat phase in order to minimize the number of nodes in the topometric map. In this work, the localization was done using a 3D lidar. Following a similar idea, Boniardi, Caselitz, Kummerle, and Burgard (2017) have extended this work to allow using architectural floor plans of buildings to localize within using 2D lidar scans. Our work differs from previous work on LT&R mainly because the system is deployed in an unstructured, outdoor environment and subject to harsh winter conditions. We also demonstrate the performance of our LT&R system on 22 km of autonomous path repeating.

3 System description

This section will present a detailed description of our LT&R system. Our system was designed to work by using 3D lidar scans as a primary mean of localization, also using IMU and wheel odometry as input. The main components of the framework are shown in Figure 2. As the iterative closest point (ICP) algorithm is the foundation of this algorithm, our implementation of the ICP algorithm is detailed first. Next, the teach phase is described, explaining how the reference trajectory and map are logged. Subsequently, the repeat phase is described, when the robot localizes within

the map a simple controller allows computing commands that allow to repeat the reference trajectory. Finally, the hardware used to deploy the LT&R system, including the UGV, sensing and computing hardware is described.
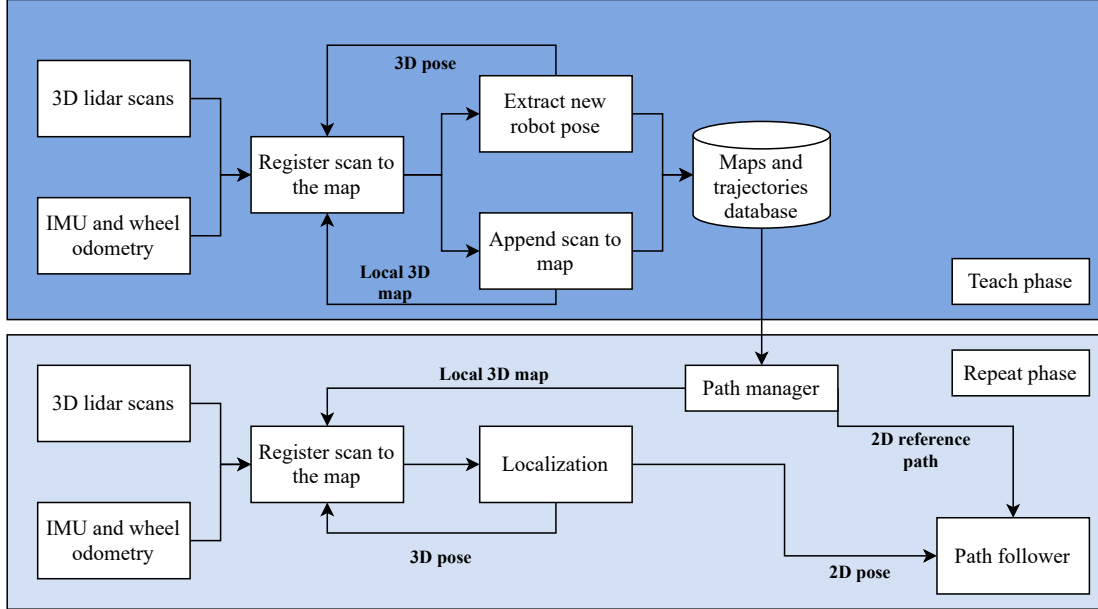

Figure 2: Flowchart for LTR

Various coordinate frames need to be defined for the LT&R framework to work, all of which are illustrated in Figure 3. First, a map frame $\mathcal{M}$ is defined representing the world in which the robot is navigating. Second, an odom frame $\mathcal{O}$ is defined in order to localize the robot at a higher frequency. The rigid transform between from the odom frame $\mathcal{O}$ to the map frame A robot frame $\mathcal{R}$ is defined at the base of the robot chassis. The rigid transform from the odom frame to the map frame $^{\mathcal{M}}_{\mathcal{O}}T$ is updated every time a new localization is computed by the ICP algorithm. Thirdly, a robot frame $\mathcal{R}$ is defined with its origin at the base of the robot chassis and the x-axis parallel to the longitudinal direction and the y-axis parallel to the lateral direction of the vehicle. The rigid transform $^{\mathcal{O}}_{\mathcal{R}}T$ is updated at the rate of the IMU and wheel odometry and used as a prior for the ICP algorithm. Fourthly, a lidar frame $\mathcal{L}$ is defined at the origin of the lidar sensor. The rigid transform from the lidar frame to the robot frame $^{\mathcal{R}}_{\mathcal{L}}T$ is assumed to be constant and found through system calibration. Reading point clouds $\mathcal{P}$ are originally observed in the lidar frame $\mathcal{L}$ but are then expressed in the map frame $\mathcal{M}$ by chaining rigid transformations from the lidar frame to the map frame $^{\mathcal{M}}_{\mathcal{L}}T$.
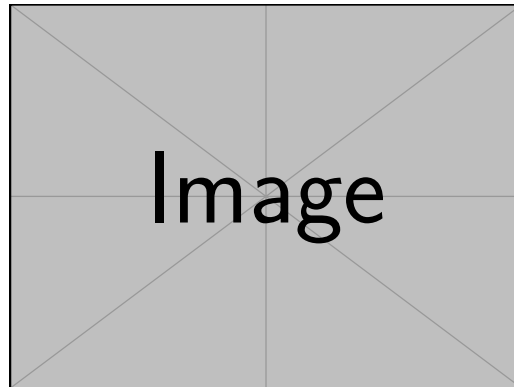

Figure 3: Coordinate frames used for LT&R

3.1 Iterative closest point

Incoming lidar scans, or reading point clouds $\mathcal{P}$ registered to a reference map, or reference point cloud $\mathcal{Q}$ using the ICP algorithm in order to localize the robot and build a map of the environment during the teach phase.
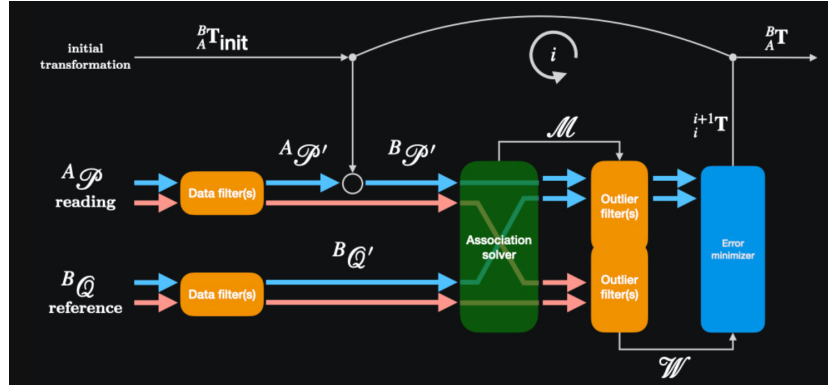

Figure 4: ICP pipeline

3.1.1 Tiled mapping for large scale

Lorem ipsum dolor sit amet, consectetuer adipiscing elit. Ut purus elit, vestibulum ut, placerat ac, adipiscing vitae, felis. Curabitur dictum gravida mauris. Nam arcu libero, nonummy eget, consectetuer id, vulputate a, magna. Donec vehicula augue eu neque. Pellentesque habitant morbi tristique senectus et netus et malesuada fames ac turpis egestas. Mauris ut leo. Cras viverra metus rhoncus sem. Nulla et lectus vestibulum urna fringilla ultrices. Phasellus eu tellus sit amet tortor gravida placerat. Integer sapien est, iaculis in, pretium quis, viverra ac, nunc. Praesent eget sem vel leo ultrices bibendum. Aenean faucibus. Morbi dolor nulla, malesuada eu, pulvinar at, mollis ac, nulla. Curabitur auctor semper nulla. Donec varius orci eget risus. Duis nibh mi, congue eu, accumsan eleifend, sagittis quis, diam. Duis eget orci sit amet orci dignissim rutrum.
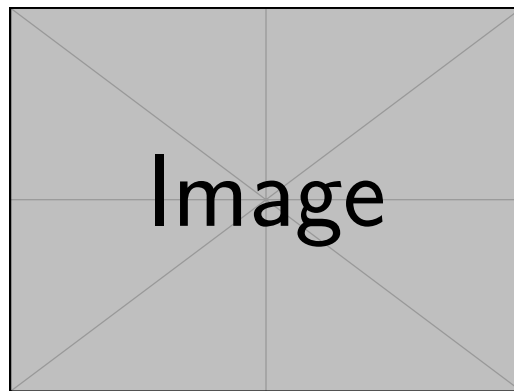

Figure 5: Figure explaining Simon-Pierre's tiled mapping framework

3.2 Teach phase

During the teach phase Lorem ipsum dolor sit amet, consectetuer adipiscing elit. Ut purus elit, vestibulum ut, placerat ac, adipiscing vitae, felis. Curabitur dictum gravida mauris. Nam arcu libero, nonummy eget, consectetuer id, vulputate a, magna. Donec vehicula augue eu neque. Pellentesque habitant morbi tristique senectus et netus et malesuada fames ac turpis egestas. Mauris ut leo. Cras viverra metus rhoncus sem. Nulla et lectus vestibulum urna fringilla

Table 1: ICP parameters

	k_g	k_o	c_3	c_4	c_5
Careful/Sparse	0.334	0.597	1.101	9.621	8.170
Careful/Dense	3.124	3.195	1.094	5.899	7.318
Aggressive/Sparse	0.840	9.153	2.853	8.274	0.187
Aggressive/Dense	4.838	2.841	0.670	7.952	0.386
Hand-Tuned	0.767	0.060	0.340	2.000	0.250

ultrices. Phasellus eu tellus sit amet tortor gravida placerat. Integer sapien est, iaculis in, pretium quis, viverra ac, nunc. Praesent eget sem vel leo ultrices bibendum. Aenean faucibus. Morbi dolor nulla, malesuada eu, pulvinar at, mollis ac, nulla. Curabitur auctor semper nulla. Donec varius orci eget risus. Duis nibh mi, congue eu, accumsan eleifend, sagittis quis, diam. Duis eget orci sit amet orci dignissim rutrum.
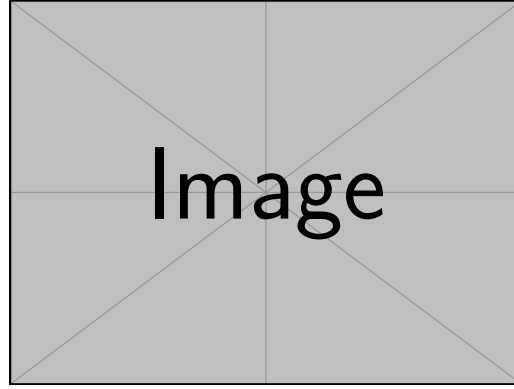

Figure 6: Teach phase pipeline

3.3 Repeat phase

Lorem ipsum dolor sit amet, consectetuer adipiscing elit. Ut purus elit, vestibulum ut, placerat ac, adipiscing vitae, felis. Curabitur dictum gravida mauris. Nam arcu libero, nonummy eget, consectetuer id, vulputate a, magna. Donec vehicula augue eu neque. Pellentesque habitant morbi tristique senectus et netus et malesuada fames ac turpis egestas. Mauris ut leo. Cras viverra metus rhoncus sem. Nulla et lectus vestibulum urna fringilla ultrices. Phasellus eu tellus sit amet tortor gravida placerat. Integer sapien est, iaculis in, pretium quis, viverra ac, nunc. Praesent eget sem vel leo ultrices bibendum. Aenean faucibus. Morbi dolor nulla, malesuada eu, pulvinar at, mollis ac, nulla. Curabitur auctor semper nulla. Donec varius orci eget risus. Duis nibh mi, congue eu, accumsan eleifend, sagittis quis, diam. Duis eget orci sit amet orci dignissim rutrum.

3.3.1 Repeat localization

Lorem ipsum dolor sit amet, consectetuer adipiscing elit. Ut purus elit, vestibulum ut, placerat ac, adipiscing vitae, felis. Curabitur dictum gravida mauris. Nam arcu libero, nonummy eget, consectetuer id, vulputate a, magna. Donec vehicula augue eu neque. Pellentesque habitant morbi tristique senectus et netus et malesuada fames ac turpis egestas. Mauris ut leo. Cras viverra metus rhoncus sem. Nulla et lectus vestibulum urna fringilla ultrices. Phasellus eu tellus sit amet tortor gravida placerat. Integer sapien est, iaculis in, pretium quis, viverra ac, nunc. Praesent eget sem vel leo ultrices bibendum. Aenean faucibus. Morbi dolor nulla, malesuada eu, pulvinar at, mollis ac, nulla. Curabitur auctor semper nulla. Donec varius orci eget risus. Duis nibh mi, congue eu, accumsan eleifend, sagittis quis, diam. Duis eget orci sit amet orci dignissim rutrum.
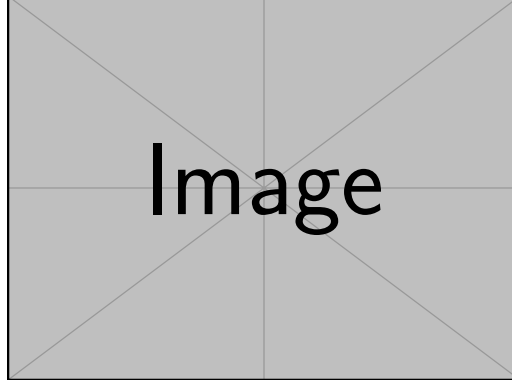
Figure 7: Repeat phase pipeline

3.3.2 Path following

Once the robot is localized within the environment and the reference trajectory is defined, this information is used as input to a simple path following controller in order to complete the repeat pipeline. The output of the path-following algorithm is the commanded longitudinal and angular velocities, defined in the vector $\boldsymbol{u} = [v_x, \omega]$. For our implementation, we selected a simple Orthogonal-Exponential (ORTHEXP) controller was selected. Originally proposed by Mojaev and Zell (2004) for differential-drive mobile robots, this controller allows path tracking with a feedback loop on robot localization. This controller was later adapted for omnidirectional mobile robots by Li, Wang, and Zell (2007) and for dribbling control for soccer robots. More recently, Huskić, Buck, and Zell (2017) improved the algorithm's path following performance through heuristic linear velocity control. To implement this controller, we used the open-source Generic Robot Navigation (GeRoNa) library, created by Huskić, Buck, and Zell (2019).

Knowing the robot's 2D pose $\boldsymbol{x}_{2D}$ and reference trajectory $\boldsymbol{x}_{ref}$, it is possible to compute the orthogonal projection $\boldsymbol{P}$ of the robot on the reference path. A path reference frame $\mathcal{X}$ is defined within the map frame with it's origin corresponding to the point $\boldsymbol{P}$. For the path reference frame, abscissa $\boldsymbol{x}_t$ and ordinate $\boldsymbol{x}_n$ are unit tangent and unit normal vectors respectively. The orthogonal distance from the origin of the robot frame $\mathcal{R}$ and the path frame $\mathcal{X}$ along the $\boldsymbol{x}_n$ axis is denoted with x_n and the tangential distance with x_t. The tangential angle of the path frame $\mathcal{X}$ with respect to the map frame $\mathcal{M}$ is defined as θ_t. The angle of robot frame $\mathcal{R}$'s $\boldsymbol{x}$ axis with respect to the map frame $\mathcal{M}$ is defined θ_r. If we denote x_{n_o} as the distance between the origin of the robot frame $\mathcal{R}$ and the origin of the path frame $\mathcal{X}$, it is possible to define the following exponential law

$$x_n = x_{n_o} e^{-kx_t} \tag{1}$$

where k is a positive constant that allows to regulate the convergence speed of the robot to the path. Next, the exponential function's tangent angle with the map frame ϕ_e can be computed as follows

$$\phi_e = \arctan(-kx_n) \tag{2}$$

A PD controller can then be defined to compute the commanded angular velocity ω with ϕ_e as error input

$$\omega = K_h(K_p\phi_e + K_d\frac{d\phi_e}{dt}) \tag{3}$$

where K_p and K_d are proportional and derivative gains. The K_h parameter is a gain on commanded angular velocity that was added after we empirically observed that the robot stabilizes at an angular velocity significantly lower than

the commanded angular velocity, based on IMU measurements. A summary of the geometrical representation of the variables affecting the angular velocity command is shown in Figure 8.
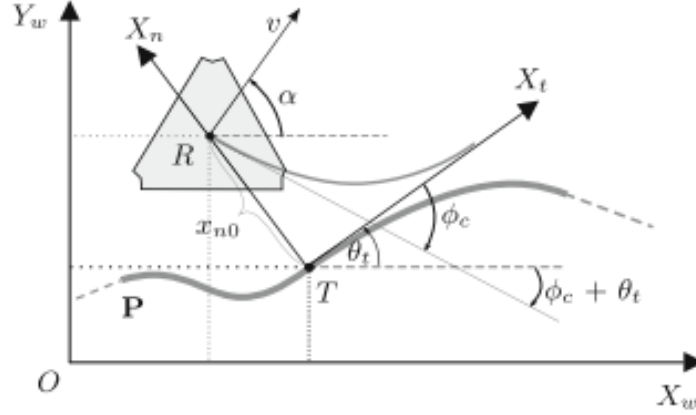

Figure 8: Figure explaining Differential orthogonal-exponential controller

In the GeRoNa library, commanded longitudinal velocity v_x can be computed based on multiple factors such as upcoming path curvature, current vehicle angular velocity, proximity of obstacles and distance from the end goal.

Table 2: ORTHEXP controller parameters

	k_g	k_o	c_3	c_4	c_5
Careful/Sparse	0.334	0.597	1.101	9.621	8.170
Careful/Dense	3.124	3.195	1.094	5.899	7.318
Aggressive/Sparse	0.840	9.153	2.853	8.274	0.187
Aggressive/Dense	4.838	2.841	0.670	7.952	0.386
Hand-Tuned	0.767	0.060	0.340	2.000	0.250

3.4 Hardware description

Our system was deployed on a Clearpath Robotics Warthog UGV. The Warthog is a SSMR using two drive units located on each side of it's chassis. For SSMRs, steering is done by sending rotating the wheels on each side of the vehicle at different velocities to creating a skidding effect, effectively turning the vehicle. The Warthog can be equipped with wheels or tracks, for this work, we selected the latter in order to maximize mobility. The Warthog is also equipped with a differential suspension, maximizing track or wheel traction when navigating steep terrain. The warthog is also equipped with a standard sensor suite for autonomous navigation. In order to enable the LT&R framework, a Robosense RS-32 3D lidar is mounted in front of the robot, for this work, it is the only lidar used for localization. 3 Hall effect sensors are added to each motor to provide wheel odometry for the robot. Finally, an XSens MTi-10 IMU provides angular velocity, body linear acceleration and gravitational acceleration measurements. Additional sensors used for recording in this work include a Dalsa C1920 camera and two Emlid Reach-RS+ GPS receivers. Two Robosense RS-16 lidars were added to the rear of the platform to collect measurements on tree canopy but no data was recorded through those sensors. All technical specifications for the platform are given in Table 3.

Table 3: Warthog specifications

Physical		**Power**	
Mass	590 kg	Chemistry	AGM sealed lead acid
Footprint	2.13 x 1.52 m	Voltage	48 V
Top speed	18 km/h	Capacity	105 Ah
Steering geometry	Skid-steering	Drive	Sevcon Gen4
Locomotion	CAMSO ATV T4S Tracks		
Suspension	Geometric Passive Articulation		
Sensors		**Computing**	
LT&R		Computer	Acrosser AIV-Q170V1FL
Front lidar	Robosense RS-32 (10 Hz)	CPU	i7-6700 TE
IMU	XSens MTi-10 (100 Hz)		
Wheel encoders	3 x hall effect sensors (4 Hz)		
Recording			
Camera	Dalsa C1920 (8 Hz)		
GPS	Emlid Reach-RS+ (5 Hz)		

Figure 9: The experimental setup for LT&R on our Clearpath Robotics Warthog UGV: (1) Robosense RS-32 lidar, (2) XSens MTi-10 IMU, (3) Acrosser AIV-Q170V1FL computer, (4) Dalsa C1920 color camera, (5) 2 Emlid Reach-RS+ GPS antennas.

4 Environment

Lorem ipsum dolor sit amet, consectetuer adipiscing elit. Ut purus elit, vestibulum ut, placerat ac, adipiscing vitae, felis. Curabitur dictum gravida mauris. Nam arcu libero, nonummy eget, consectetuer id, vulputate a, magna. Donec vehicula augue eu neque. Pellentesque habitant morbi tristique senectus et netus et malesuada fames ac turpis egestas. Mauris ut leo. Cras viverra metus rhoncus sem. Nulla et lectus vestibulum urna fringilla ultrices. Phasellus eu tellus sit amet tortor gravida placerat. Integer sapien est, iaculis in, pretium quis, viverra ac, nunc. Praesent eget sem vel leo ultrices bibendum. Aenean faucibus. Morbi dolor nulla, malesuada eu, pulvinar at, mollis ac, nulla. Curabitur auctor semper nulla. Donec varius orci eget risus. Duis nibh mi, congue eu, accumsan eleifend, sagittis quis, diam. Duis eget orci sit amet orci dignissim rutrum.
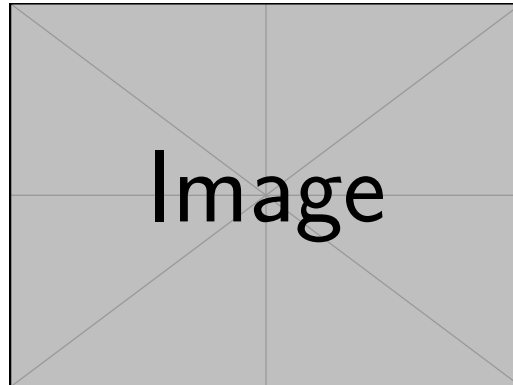

Figure 10: Johann's various runs and meteo figure

Lorem ipsum dolor sit amet, consectetuer adipiscing elit. Ut purus elit, vestibulum ut, placerat ac, adipiscing vitae, felis. Curabitur dictum gravida mauris. Nam arcu libero, nonummy eget, consectetuer id, vulputate a, magna. Donec vehicula augue eu neque. Pellentesque habitant morbi tristique senectus et netus et malesuada fames ac turpis egestas. Mauris ut leo. Cras viverra metus rhoncus sem. Nulla et lectus vestibulum urna fringilla ultrices. Phasellus eu tellus sit amet tortor gravida placerat. Integer sapien est, iaculis in, pretium quis, viverra ac, nunc. Praesent eget sem vel leo ultrices bibendum. Aenean faucibus. Morbi dolor nulla, malesuada eu, pulvinar at, mollis ac, nulla. Curabitur auctor semper nulla. Donec varius orci eget risus. Duis nibh mi, congue eu, accumsan eleifend, sagittis quis, diam. Duis eget orci sit amet orci dignissim rutrum.

5 Results

Lorem ipsum dolor sit amet, consectetuer adipiscing elit. Ut purus elit, vestibulum ut, placerat ac, adipiscing vitae, felis. Curabitur dictum gravida mauris. Nam arcu libero, nonummy eget, consectetuer id, vulputate a, magna. Donec vehicula augue eu neque. Pellentesque habitant morbi tristique senectus et netus et malesuada fames ac turpis egestas. Mauris ut leo. Cras viverra metus rhoncus sem. Nulla et lectus vestibulum urna fringilla ultrices. Phasellus eu tellus sit amet tortor gravida placerat. Integer sapien est, iaculis in, pretium quis, viverra ac, nunc. Praesent eget sem vel leo ultrices bibendum. Aenean faucibus. Morbi dolor nulla, malesuada eu, pulvinar at, mollis ac, nulla. Curabitur auctor semper nulla. Donec varius orci eget risus. Duis nibh mi, congue eu, accumsan eleifend, sagittis quis, diam. Duis eget orci sit amet orci dignissim rutrum.

5.1 Localization

Lorem ipsum dolor sit amet, consectetuer adipiscing elit. Ut purus elit, vestibulum ut, placerat ac, adipiscing vitae, felis. Curabitur dictum gravida mauris. Nam arcu libero, nonummy eget, consectetuer id, vulputate a, magna. Donec vehicula augue eu neque. Pellentesque habitant morbi tristique senectus et netus et malesuada fames ac turpis egestas.

Mauris ut leo. Cras viverra metus rhoncus sem. Nulla et lectus vestibulum urna fringilla ultrices. Phasellus eu tellus sit amet tortor gravida placerat. Integer sapien est, iaculis in, pretium quis, viverra ac, nunc. Praesent eget sem vel leo ultrices bibendum. Aenean faucibus. Morbi dolor nulla, malesuada eu, pulvinar at, mollis ac, nulla. Curabitur auctor semper nulla. Donec varius orci eget risus. Duis nibh mi, congue eu, accumsan eleifend, sagittis quis, diam. Duis eget orci sit amet orci dignissim rutrum.
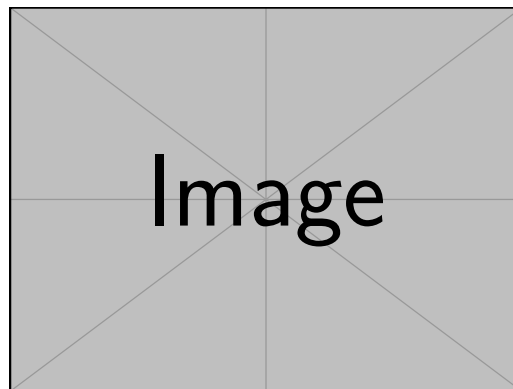
5.1.1 Vision-based

Lorem ipsum dolor sit amet, consectetuer adipiscing elit. Ut purus elit, vestibulum ut, placerat ac, adipiscing vitae, felis. Curabitur dictum gravida mauris. Nam arcu libero, nonummy eget, consectetuer id, vulputate a, magna. Donec vehicula augue eu neque. Pellentesque habitant morbi tristique senectus et netus et malesuada fames ac turpis egestas. Mauris ut leo. Cras viverra metus rhoncus sem. Nulla et lectus vestibulum urna fringilla ultrices. Phasellus eu tellus sit amet tortor gravida placerat. Integer sapien est, iaculis in, pretium quis, viverra ac, nunc. Praesent eget sem vel leo ultrices bibendum. Aenean faucibus. Morbi dolor nulla, malesuada eu, pulvinar at, mollis ac, nulla. Curabitur auctor semper nulla. Donec varius orci eget risus. Duis nibh mi, congue eu, accumsan eleifend, sagittis quis, diam. Duis eget orci sit amet orci dignissim rutrum.

Figure 11: Olivier's over and under exposition figure for cameras

5.1.2 GNSS

Lorem ipsum dolor sit amet, consectetuer adipiscing elit. Ut purus elit, vestibulum ut, placerat ac, adipiscing vitae, felis. Curabitur dictum gravida mauris. Nam arcu libero, nonummy eget, consectetuer id, vulputate a, magna. Donec vehicula augue eu neque. Pellentesque habitant morbi tristique senectus et netus et malesuada fames ac turpis egestas. Mauris ut leo. Cras viverra metus rhoncus sem. Nulla et lectus vestibulum urna fringilla ultrices. Phasellus eu tellus sit amet tortor gravida placerat. Integer sapien est, iaculis in, pretium quis, viverra ac, nunc. Praesent eget sem vel leo ultrices bibendum. Aenean faucibus. Morbi dolor nulla, malesuada eu, pulvinar at, mollis ac, nulla. Curabitur auctor semper nulla. Donec varius orci eget risus. Duis nibh mi, congue eu, accumsan eleifend, sagittis quis, diam. Duis eget orci sit amet orci dignissim rutrum.

5.1.3 ICP

Lorem ipsum dolor sit amet, consectetuer adipiscing elit. Ut purus elit, vestibulum ut, placerat ac, adipiscing vitae, felis. Curabitur dictum gravida mauris. Nam arcu libero, nonummy eget, consectetuer id, vulputate a, magna. Donec vehicula augue eu neque. Pellentesque habitant morbi tristique senectus et netus et malesuada fames ac turpis egestas. Mauris ut leo. Cras viverra metus rhoncus sem. Nulla et lectus vestibulum urna fringilla ultrices. Phasellus eu tellus sit amet tortor gravida placerat. Integer sapien est, iaculis in, pretium quis, viverra ac, nunc. Praesent eget sem vel leo ultrices bibendum. Aenean faucibus. Morbi dolor nulla, malesuada eu, pulvinar at, mollis ac, nulla. Curabitur auctor
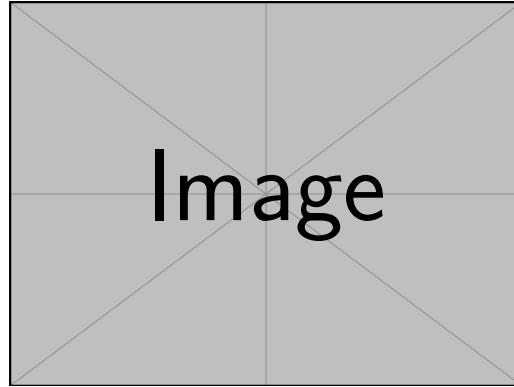
Figure 12: Maxime's GNSS error figure

semper nulla. Donec varius orci eget risus. Duis nibh mi, congue eu, accumsan eleifend, sagittis quis, diam. Duis eget orci sit amet orci dignissim rutrum.
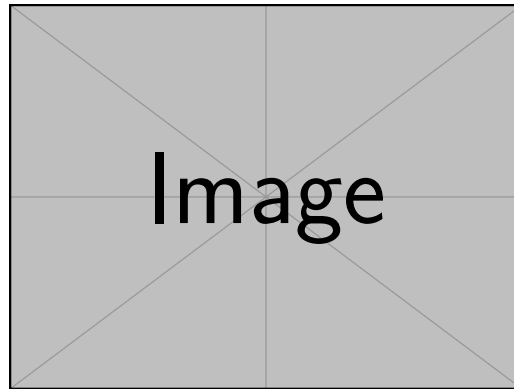

Figure 13: Figure explaining ICP error for every run (correlated with meteo).

5.2   Motion and control

Lorem ipsum dolor sit amet, consectetuer adipiscing elit. Ut purus elit, vestibulum ut, placerat ac, adipiscing vitae, felis. Curabitur dictum gravida mauris. Nam arcu libero, nonummy eget, consectetuer id, vulputate a, magna. Donec vehicula augue eu neque. Pellentesque habitant morbi tristique senectus et netus et malesuada fames ac turpis egestas. Mauris ut leo. Cras viverra metus rhoncus sem. Nulla et lectus vestibulum urna fringilla ultrices. Phasellus eu tellus sit amet tortor gravida placerat. Integer sapien est, iaculis in, pretium quis, viverra ac, nunc. Praesent eget sem vel leo ultrices bibendum. Aenean faucibus. Morbi dolor nulla, malesuada eu, pulvinar at, mollis ac, nulla. Curabitur auctor semper nulla. Donec varius orci eget risus. Duis nibh mi, congue eu, accumsan eleifend, sagittis quis, diam. Duis eget orci sit amet orci dignissim rutrum.

5.2.1   Path following error

Lorem ipsum dolor sit amet, consectetuer adipiscing elit. Ut purus elit, vestibulum ut, placerat ac, adipiscing vitae, felis. Curabitur dictum gravida mauris. Nam arcu libero, nonummy eget, consectetuer id, vulputate a, magna. Donec vehicula augue eu neque. Pellentesque habitant morbi tristique senectus et netus et malesuada fames ac turpis egestas. Mauris ut leo. Cras viverra metus rhoncus sem. Nulla et lectus vestibulum urna fringilla ultrices. Phasellus eu tellus sit amet tortor gravida placerat. Integer sapien est, iaculis in, pretium quis, viverra ac, nunc. Praesent eget sem vel leo ultrices bibendum. Aenean faucibus. Morbi dolor nulla, malesuada eu, pulvinar at, mollis ac, nulla. Curabitur auctor
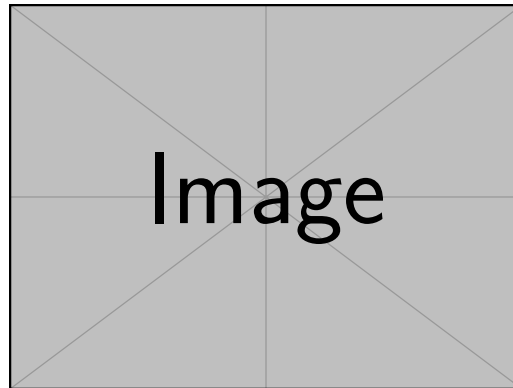
Figure 14: Figure explaining special cases when mapping needed to be enabled.

semper nulla. Donec varius orci eget risus. Duis nibh mi, congue eu, accumsan eleifend, sagittis quis, diam. Duis eget orci sit amet orci dignissim rutrum.
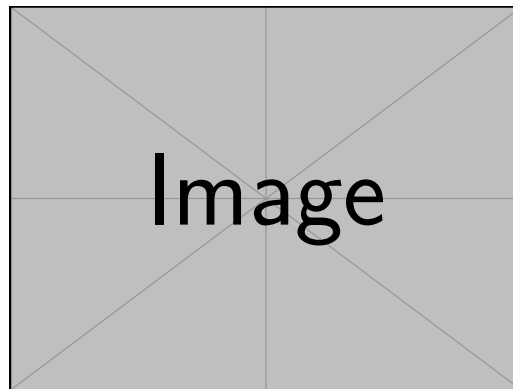

Figure 15: Dominic's path following error figure

5.2.2 Command error and power consumption

Lorem ipsum dolor sit amet, consectetuer adipiscing elit. Ut purus elit, vestibulum ut, placerat ac, adipiscing vitae, felis. Curabitur dictum gravida mauris. Nam arcu libero, nonummy eget, consectetuer id, vulputate a, magna. Donec vehicula augue eu neque. Pellentesque habitant morbi tristique senectus et netus et malesuada fames ac turpis egestas. Mauris ut leo. Cras viverra metus rhoncus sem. Nulla et lectus vestibulum urna fringilla ultrices. Phasellus eu tellus sit amet tortor gravida placerat. Integer sapien est, iaculis in, pretium quis, viverra ac, nunc. Praesent eget sem vel leo ultrices bibendum. Aenean faucibus. Morbi dolor nulla, malesuada eu, pulvinar at, mollis ac, nulla. Curabitur auctor semper nulla. Donec varius orci eget risus. Duis nibh mi, congue eu, accumsan eleifend, sagittis quis, diam. Duis eget orci sit amet orci dignissim rutrum.

6 Lessons learned

Lorem ipsum dolor sit amet, consectetuer adipiscing elit. Ut purus elit, vestibulum ut, placerat ac, adipiscing vitae, felis. Curabitur dictum gravida mauris. Nam arcu libero, nonummy eget, consectetuer id, vulputate a, magna. Donec vehicula augue eu neque. Pellentesque habitant morbi tristique senectus et netus et malesuada fames ac turpis egestas. Mauris ut leo. Cras viverra metus rhoncus sem. Nulla et lectus vestibulum urna fringilla ultrices. Phasellus eu tellus sit amet tortor gravida placerat. Integer sapien est, iaculis in, pretium quis, viverra ac, nunc. Praesent eget sem vel leo
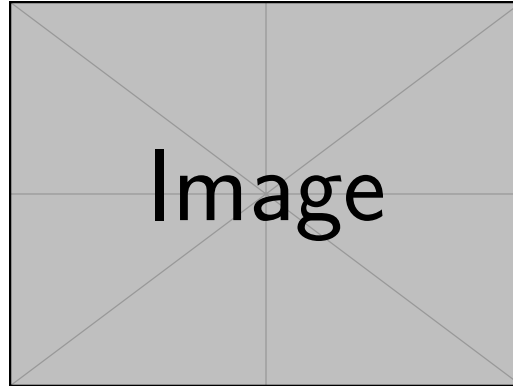
Figure 16: Power consumption / motion efficiency figure.

ultrices bibendum. Aenean faucibus. Morbi dolor nulla, malesuada eu, pulvinar at, mollis ac, nulla. Curabitur auctor semper nulla. Donec varius orci eget risus. Duis nibh mi, congue eu, accumsan eleifend, sagittis quis, diam. Duis eget orci sit amet orci dignissim rutrum.

Lorem ipsum dolor sit amet, consectetuer adipiscing elit. Ut purus elit, vestibulum ut, placerat ac, adipiscing vitae, felis. Curabitur dictum gravida mauris. Nam arcu libero, nonummy eget, consectetuer id, vulputate a, magna. Donec vehicula augue eu neque. Pellentesque habitant morbi tristique senectus et netus et malesuada fames ac turpis egestas. Mauris ut leo. Cras viverra metus rhoncus sem. Nulla et lectus vestibulum urna fringilla ultrices. Phasellus eu tellus sit amet tortor gravida placerat. Integer sapien est, iaculis in, pretium quis, viverra ac, nunc. Praesent eget sem vel leo ultrices bibendum. Aenean faucibus. Morbi dolor nulla, malesuada eu, pulvinar at, mollis ac, nulla. Curabitur auctor semper nulla. Donec varius orci eget risus. Duis nibh mi, congue eu, accumsan eleifend, sagittis quis, diam. Duis eget orci sit amet orci dignissim rutrum.

7   Conclusion

Lorem ipsum dolor sit amet, consectetuer adipiscing elit. Ut purus elit, vestibulum ut, placerat ac, adipiscing vitae, felis. Curabitur dictum gravida mauris. Nam arcu libero, nonummy eget, consectetuer id, vulputate a, magna. Donec vehicula augue eu neque. Pellentesque habitant morbi tristique senectus et netus et malesuada fames ac turpis egestas. Mauris ut leo. Cras viverra metus rhoncus sem. Nulla et lectus vestibulum urna fringilla ultrices. Phasellus eu tellus sit amet tortor gravida placerat. Integer sapien est, iaculis in, pretium quis, viverra ac, nunc. Praesent eget sem vel leo ultrices bibendum. Aenean faucibus. Morbi dolor nulla, malesuada eu, pulvinar at, mollis ac, nulla. Curabitur auctor semper nulla. Donec varius orci eget risus. Duis nibh mi, congue eu, accumsan eleifend, sagittis quis, diam. Duis eget orci sit amet orci dignissim rutrum.

References

Bares, J. E. & Wettergreen, D. S. (1999). Dante II: Technical Description, Results, and Lessons Learned. *The International Journal of Robotics Research*, *18*(7), 621–649.

Apostolopoulos, D. S., Wagner, M. D., Shamah, B. N., Pedersen, L., Shillcutt, K., & Whittaker, W. L. (2000). Technology and Field Demonstration of Robotic Search for Antarctic Meteorites. *The International Journal of Robotics Research*, *19*(11), 1015–1032.

Moorehead, S., Simmons, R., Apostolopoulos, D. (, & Whittaker, W. (L. (1999). Autonomous navigation field results of a planetary analog robot in antarctica. In *Proceedings of international symposium on artificial intelligence, robotics and automation in space (isairas '99).*

Stansbury, R. S., Akers, E. L., Harmon, H. P., & Agah, A. (2004). Survivability, mobility, and functionality of a rover for radars in polar regions. *International Journal of Control, Automation and Systems*, *2*(3), 343–353.

Gifford, C. M., Akers, E. L., Stansbury, R. S., & Agah, A. (2009). Mobile Robots for Polar Remote Sensing. In *The path to autonomous robots* (pp. 1–22). Boston, MA: Springer US.

Williams, S. & Howard, A. M. (2009). Developing monocular visual pose estimation for arctic environments. *Journal of Field Robotics*, *27*(2), 145–157.

Williams, S. & Howard, A. M. (2010). Towards Visual Arctic Terrain Assessment. In *Springer tracts in advanced robotics* (Vol. 62, pp. 91–100). Springer.

Williams, S. & Howard, A. M. (2011). Horizon line estimation in glacial environments using multiple visual cues. *Proceedings - IEEE International Conference on Robotics and Automation*, 5887–5892.

Lever, J. H., Delaney, A. J., Ray, L. E., Trautmann, E., Barna, L. A., & Burzynski, A. M. (2013). Autonomous GPR Surveys using the Polar Rover Yeti. *Journal of Field Robotics*, *30*(2), 194–215.

Paton, M., Pomerleau, F., MacTavish, K., Ostafew, C. J., & Barfoot, T. D. (2017). Expanding the Limits of Vision-based Localization for Long-term Route-following Autonomy. *Journal of Field Robotics*, *34*(1), 98–122.

Ort, T., Gilitschenski, I., & Rus, D. (2020). Autonomous navigation in inclement weather based on a localizing ground penetrating radar. *IEEE Robotics and Automation Letters*, *5*(2), 3267–3274.

Furgale, P. & Barfoot, T. D. (2010). Visual teach and repeat for long-range rover autonomy. *Journal of Field Robotics*, *27*(5), 534–560.

Churchill, W. & Newman, P. (2013). Experience-based navigation for long-term localisation. *The International Journal of Robotics Research*, *32*(14), 1645–1661.

Paton, M., MacTavish, K., Warren, M., & Barfoot, T. D. (2016). Bridging the appearance gap: Multi-experience localization for long-term visual teach and repeat. In *2016 ieee/rsj international conference on intelligent robots and systems (iros)* (Vol. 2016-Novem, pp. 1918–1925). IEEE.

MacTavish, K., Paton, M., & Barfoot, T. D. (2017). Visual triage: A bag-of-words experience selector for long-term visual route following. In *2017 ieee international conference on robotics and automation (icra)* (pp. 2065–2072). IEEE.

Paton, M., MacTavish, K., Ostafew, C. J., & Barfoot, T. D. (2015). It's not easy seeing green: Lighting-resistant stereo Visual Teach & Repeat using color-constant images. *Proceedings - IEEE International Conference on Robotics and Automation*, *2015-June*(June), 1519–1526.

McManus, C., Furgale, P., Stenning, B., & Barfoot, T. D. (2013). Lighting-invariant visual teach and repeat using appearance-based lidar. *Journal of Field Robotics*, *30*(2), 254–287.

Clement, L., Kelly, J., & Barfoot, T. D. (2017). Robust Monocular Visual Teach and Repeat Aided by Local Ground Planarity and Color-constant Imagery. *Journal of Field Robotics*, *34*(1), 74–97.

Camara, L. G., Pivonka, T., Jilek, M., Gabert, C., Kosnar, K., & Preucil, L. (2020). Accurate and Robust Teach and Repeat Navigation by Visual Place Recognition: A CNN Approach. *IEEE International Conference on Intelligent Robots and Systems*, 6018–6024.

Congram, B. & Barfoot, T. D. (2021). Relatively Lazy: Indoor-Outdoor Navigation Using Vision and GNSS.

Marshall, J., Barfoot, T., & Larsson, J. (2008). Autonomous underground tramming for center-articulated vehicles. *Journal of Field Robotics*, *25*(6-7), 400–421.

Sprunk, C., Tipaldi, G. D., Cherubini, A., & Burgard, W. (2013). Lidar-based teach-and-repeat of mobile robot trajectories. *IEEE International Conference on Intelligent Robots and Systems*, 3144–3149.

Mazuran, M., Sprunk, C., Burgard, W., & Tipaldi, G. D. (2015). LexTOR: Lexicographic teach optimize and repeat based on user preferences. *Proceedings - IEEE International Conference on Robotics and Automation*, *2015-June*(June), 2780–2786.

Landry, D. & Giguère, P. (2016). Automating node pruning for LiDAR-based topometric maps in the context of teach-and-repeat. *Proceedings - 2016 13th Conference on Computer and Robot Vision, CRV 2016*, 132–139.

Boniardi, F., Caselitz, T., Kummerle, R., & Burgard, W. (2017). Robust LiDAR-based localization in architectural floor plans. *IEEE International Conference on Intelligent Robots and Systems*, *2017-September*, 3318–3324.

Mojaev, A. & Zell, A. (2004). Tracking Control and Adaptive Local Navigation for Nonholonomic Mobile Robot. *Intelligent Autonomous Systems (IAS-8)*, 521–528.

Li, X., Wang, M., & Zell, A. (2007). Dribbling Control of Omnidirectional Soccer Robots. In *Proceedings 2007 ieee international conference on robotics and automation* (April, pp. 2623–2628). IEEE.

Huskić, G., Buck, S., & Zell, A. (2017). A Simple and Efficient Path Following Algorithm for Wheeled Mobile Robots. In *Advances in intelligent systems and computing* (Vol. 531, pp. 375–387).

Huskić, G., Buck, S., & Zell, A. (2019). GeRoNa: Generic Robot Navigation. *Journal of Intelligent & Robotic Systems*, *95*(2), 419–442.